TITLE: ANALYSIS OF AUGMENTATION IN PERFORMANCE OF PV MODULE INTEGRATED

WITH FINNED PCM BY THREE-DIMENSIONAL TRANSIENT NUMERICAL SIMULATION

AUTHORS: Unnikrishnan K S,Sumanth Babu Pathipati,Rohinikumar Bandaru

PAGES: 143-162

ORIGINAL PDF URL: https://dergipark.org.tr/tr/download/article-file/3975227

ANALYSIS OF AUGMENTATION IN PERFORMANCE OF PV MODULE INTEGRATED WITH FINNED PCM BY THREE-DIMENSIONAL TRANSIENT NUMERICAL SIMULATION

K.S. UNNIKRISHNAN*, Sumanth Babu PATHIPATI**, Rohinikumar BANDARU***

* National Institute of Technology Calicut, Department of Mechanical Engineering,
673601 Kozhikode, India, kgsunnikrishnan@gmail.com ORCID: 0000-0002-2231-5391
** National Institute of Technology Calicut, Department of Mechanical Engineering,
673601 Kozhikode, India, sumanth3a6@gmail.com ORCID: 0009-0002-3033-5349
*** National Institute of Technology Calicut, Department of Mechanical Engineering,
673601 Kozhikode, India, rohinikumar@nitc.ac.in ORCID: 0000-0002-3975-3996

Abstract: The overall performance of PV-PCM integrated with rectangular straight fins is analysed by three-dimensional transient numerical simulations. The influence of fin lengths, number of fins (n), and inclination (θ) of the system is investigated and compared with the PV-only system, and an optimal system configuration is then identified. Finite element analysis is used to conduct the simulations using COMSOL *Multiphysics* 6.0. The PV front surface is subjected to a constant flux of 1000 W/m² for 180 min, and the PCM employed is RT25HC. The results indicate that the average PV temperature tends to drop with increasing inclination and fin length, thereby enhancing the PV efficiency, with maximum improvement attained for the full fin case for a given inclination and number of fins. Compared to the PV-only system, the highest PV temperature reduction and PV efficiency enhancement are 59.65 °C and 45.1%, respectively, for the horizontal system of full-length fins with a number of fins equal to 6. The full-fin PV-PCM system with 6 fins and 45° inclination gives the highest instantaneous power output of 14.16 W. The melting rate of PCM is strongly related to the heat transfer rate inside PCM, and the lowest melting time is obtained for the 8-finned PV-PCM system with $\theta = 45°$. The peak velocity magnitude for all systems with different fin lengths is also examined to analyse the extent of convection levels within PCM.
Keywords: Transient numerical simulations, Number of fins, Inclination angle, PV efficiency, Melting rate

ÜÇ BOYUTLU GEÇİCİ SAYISAL SİMÜLASYON İLE KANATLI PCM İLE ENTEGRE PV MODÜLÜN PERFORMANSINDAKİ ARTIŞIN ANALİZİ

Özet: Dikdörtgen düz kanatlarla entegre edilmiş PV-PCM'nin genel performansı, üç boyutlu geçici sayısal simülasyonlarla analiz edilir. Sistemin kanat uzunluklarının, kanat sayısının (n) ve eğiminin (θ) etkisi araştırılır ve yalnızca PV sistemiyle karşılaştırılır ve daha sonra optimum sistem konfigürasyonu tanımlanır. Simülasyonları COMSOL *Multiphysics* 6.0 kullanarak gerçekleştirmek için sonlu elemanlar analizi kullanıldı. PV'nin ön yüzeyi 180 dakika boyunca 1000 W/m² 'lik sabit bir akışa maruz bırakılır ve kullanılan PCM, RT25HC'dir. Sonuçlar, ortalama PV sıcaklığının artan eğim ve kanat uzunluğuyla birlikte düşme eğiliminde olduğunu, dolayısıyla PV verimliliğinin arttığını ve belirli bir eğim ve kanat sayısı için tam kanat durumunda maksimum iyileştirmenin elde edildiğini göstermektedir. Yalnızca PV sistemiyle karşılaştırıldığında, kanat sayısı 6'ya eşit olan tam uzunlukta kanatlardan oluşan yatay sistem için en yüksek PV sıcaklık düşüşü ve PV verimlilik artışı sırasıyla 59,65 °C ve %45,1'dir. -6 kanatlı ve 45° eğimli PCM sistemi, 14,16 W ile en yüksek anlık güç çıkışını verir. PCM'nin erime hızı, PCM içindeki ısı aktarım hızıyla güçlü bir şekilde ilişkilidir ve en düşük erime süresi, 8 kanatlı PV- için elde edilir. $\theta = 45°$ olan PCM sistemi. Farklı kanat uzunluklarına sahip tüm sistemler için tepe hız büyüklüğü de PCM içindeki konveksiyon seviyelerinin kapsamını analiz etmek için incelenir.
Anahtar Kelimeler: Geçici rejim sayısal simülasyonlar, Kanat sayısı, Eğim açısı, PV verimliliği, Erime hızı.

NOMENCLATURE

A	Upper surface of the PV panel [m²]	η	Efficiency [%]
B	Liquid fraction	G_T	Solar irradiation [W/m²]
β	Volume expansion coefficient [K⁻¹]	γ	Temperature coefficient of PV material [K⁻¹]
c_p	Heat capacity [J/ kg.K]	g	Acceleration due to gravity [m/s²]
ΔT	Phase change zone [°C]	h	heat transfer coefficient [W/m2 .K]
		k	Thermal conductivity [W/m.K]
		L_c	Characteristic length [m]

L_h	Latent heat [J/kg]
μ	Dynamic viscosity [Pa s]
v	Kinematic viscosity [m^2/s]
P	Pressure [Pa]
Q_g	Heat generation per unit volume [W/m^3]
Ra	Rayleigh number
Re	Reynolds number
ρ	Density [kg/m^3]
T	Temperature [°C]
T_m	Melting temperature [°C]
t	Time [s]
θ	Inclination angle (°)

INTRODUCTION

Growing global power demand, rising fossil fuel prices, and global warming worries have accelerated the idea of a swift transition to renewable energy supply, particularly in the last two decades (Azarpour et al., 2013). The most abundant renewable energy source on earth is solar energy. Installing photovoltaic (PV) on the roofs of houses can reduce reliance on the electrical grid and lead to net-zero energy (Cuce and Cuce, 2014). Over the years, various methods have been developed to increase the efficiency of solar power generation and make it a more cost-effective technology (Mohanraj et al., 2016). The effectiveness of photovoltaic solar cells diminishes with the rise in their temperature, according to the experiments done by Radziemska (Hui Dai and Wei-Min Ma, 2002). The drop in open-circuit cell voltage is the primary source of the decrease in conversion efficiency of the cell, and hence, PV cells must be cooled to work efficiently during peak sunshine hours (Kaldellis et al., 2014). The commercially available PV module has 12% to 18% electric conversion efficiency. The excess solar radiation falling on the PV is converted to thermal energy, which raises the solar modules' working temperature (Agrawal and Tiwari, 2010; Dubey et al., 2013). To combat the impacts of high cell temperatures and keep the cell's operating temperature within an acceptable range, effective cooling mechanisms must be used to remove excess thermal energy by heat transfer from the cells (Ali, 2020; Bilen and Erdoğan, 2023). PCM with a proper melting temperature can be used to maintain the temperature of the PV module within the required temperature range, allowing it to achieve high efficiency. PCM provides the added benefit of storing thermal energy as compared to other passive techniques of thermal regulation (Da et al., 2023). The PCMs used are mostly organic types with very low thermal conductivity, so enhancement techniques such as the inclusion of fins are adopted for effective thermal regulation of PV (Kazem et al., 2023).

Bria et al. (2023) numerically investigated the utilisation of a PV-PCM cooling system as a means to minimise the adverse impact of temperature on the efficiency of PV with six different PCM thicknesses. The optimal PCM thickness for achieving maximum power output is found to be 0.06 m. Chibani et al. (2023) examined the integration of fins composed of different materials and explored the effects of the inclination angle of the panel. Cuce et al. (2011) studied a passively cooled silicon solar cell with a heat sink and observed a significant energy and exergy efficiency increase. The power conversion of PV increased by 13% at a solar radiation of 800 W/m^2. Experimental and numerical analyses were done by Park et al. (2014) to study the performance of a vertical PV-PCM, and the results showed that the power output rose by 1.0 to 1.5% compared to the conventional PV module.

The thermal management of a building with a concentrated PV–PCM system was investigated by Sharma et al. (2016), and a maximum improvement in electrical efficiency of 6.8% was reported for the incident radiation flux of 1200W/m^2. A transient numerical investigation of the PV-PCM system was conducted by Kant et al. (2016) by using RT35HC as PCM, and a maximum temperature reduction of 58.5 °C was found. It was reported that the increased wind speed and inclination resulted in a reduced PV panel temperature. The effects of employing several PCMs of different thicknesses and outside working conditions on PV-PCM performance were analysed by Nouira and Sammouda (2018). The results showed that the power output of PV increases with low dust deposition, increased PCM thickness, high wind speed, and low wind azimuth angle. Metwally et al. (2021) combined RT25 PCM with PV panels and found that efficiency increased by 2.5% in summer and 3.5% in normal weather.

The integration of two PCMs (PCM27 and PCM31) through an alternative tubular shape enclosure on PV was experimentally studied by Savvakis et al. (2020), and the results showed a temperature decrease of 6.4 and 7.5 °C, respectively, for PCM27 and PCM31 compared to the PV only system. Kumar et al. (2020) studied the impact of integrating PCM on the thermal behaviour and electrical performance of the panel to examine the system's behaviour. The use of PCM could lower the panel temperature by an average of 4.4 °C and boost efficiency by 2.2%. The influence of tilt angle on the melting of PCM-based heat sink and its potential usage for passive cooling of PV was examined by Abdulmunem et al. (2021). The findings demonstrated that when the tilt angle of the system increases from 0° to 90°, the PV temperature decreases from 0.4% to 12%. Akshayveer et al. (2021) explored a new bifacial PV-PCM system, which significantly increases PV electric output by about 74% compared to the PV-PCM system. According to Variji et al. (2022), incorporating metal foam with a porosity of 0.9 led to a 6.8% increase in average PV temperature and a 9.8% improvement in electrical efficiency compared to the PV-PCM system.

The impact of convection with RT27 PCM on the heat transfer rate from the PV panel in a finned PV-PCM system was investigated theoretically and experimentally by Huang et al. (2011), and they found that PCM with internal fins resulted in a reduction in the PV temperature up to 12 °C. Khanna et al. (2018) compared the performances of PV, PV-PCM, and Finned-PV-PCM systems using modelling and simulation and inferred that the PV module could be kept cooler by reducing the distance between fins, but reducing spacing below 25 cm does not improve the performance. Singh et al. (2020) proposed a mathematical model for a finned PV-PCM system. The effects of wind azimuths, ambient temperature, phase change temperature, and FPCM confinement dimensions were studied. The results showed that for 5 cm deep FPCM confinement, the power enhancement period increases from 6.1 h to 7.3 h when the wind azimuth varies from 75° to 0°. The impact of various structures of fins on the thermal performance of finned PV-PCM system oriented at various inclinations was quantitatively examined by Groulx et al. (2020) using a two-dimensional numerical study. Full fin and front fin configurations were found to be the most effective. Khanna et al. (2019) conducted a study to optimise a finned PV-PCM system for power augmentation under various operating conditions such as wind speed, azimuth angle, outdoor temperature, phase transition point, fin spacing, and fin width. A power generation of 143 W/m^2 was obtained for the system with a fin width of 4 mm, as compared to 125 W/m^2 for PV-only system.

The impact of fins in a rectangular enclosure of solid-liquid PCM on heat transfer was investigated numerically by Biwole et al. (2018). The results revealed that increasing the number of fins decreases the front surface temperature as well as the regulation period and speeds up the latent energy stored in the PCM. Emam and Ahmed (2018) computationally simulated a PV-PCM system with heat sinks in four different configurations based on the number and position of cavities and showed that a five-parallel cavity configuration significantly reduces solar cell temperature. Yıldız et al. (2020) explored the heat transfer inside a PCM container, which can serve as a typical model for PV/PCM systems, numerically, taking into account varied aspect ratios and types of fins. When the aspect ratio equals 1, the natural convection rate inside PCM is at its highest. Johnston et al. (2021) carried out a combined computational and experimental analysis to determine how orientation impacts the performance of a heat sink in a PV-PCM system and how fin height influences the heat sink's ability. Power output rose by 11.3 % and 15.3 % for PV integrated with 20 mm and 100 mm heat sinks, respectively, compared to standalone PV.

Klemm et al. (2017) numerically investigated the passive cooling of the system consisting of PCM with metallic fibre architectures using the COMSOL *Multiphysics* and found that the peak panel temperature

was reduced by around 20 K compared to the PV alone system. Duan (2021) examined the utilisation of porous PV-PCM systems with various inclinations numerically as well as experimentally and concluded that the inclination has little effect on the porous PCM system when the porosity is minimal. Based on numerical simulation, Mahdi et al. (2021) showed that the employment of multiple PCMs in a particular position may improve in liquid fraction and thermal regulation period by 18% and 33%, respectively. Additionally, combining several PCMs with acceptable thermophysical properties at lower inclinations can further reduce the PV temperature. Sasidharan and Bandaru (2022) conducted an analysis by numerical simulation of a nano-enhanced PCM (PV-NEPCM) system with mass concentrations of 1%, 3%, and 5% and compared its performance with that of a conventional PV-PCM system. It was found that NEPCM performs better at lower inclinations with a temperature drop of the PV module as 1.26 °C for horizontal orientation PV-PCM system.

From the literature, it can be concluded that the integration of PCM with a PV module is an effective way of thermal regulation of the module when PCM is incorporated with proper thermal conductivity enhancers like fins, metallic fibres and nanoparticles. It is also worth noting that practically most of the previous numerical studies related to finned PV-PCM systems have started with the assumption of the two-dimensional domain without considering the variation of temperature and velocity of PCM in the z-axis and almost all deal with its thermal performance. To this end, the novelty of the present work is that, here, a three-dimensional transient numerical model has been developed for finned PV-PCM systems to study the effect of PCM and fins on the thermal performance of the system and the electrical performance of the PV module. Modelling finned PV-PCM systems in three dimensions for numerical analysis offers several important advantages and provides a more realistic representation of the system's behaviour compared to two-dimensional models. Key reasons for the importance of 3D modelling are (1) Accurate representation of complex geometries, accounting for variations in shape, size, and positioning of components such as fins. This is critical for capturing the interactions and flow patterns within the system; (2) Realistic boundary conditions that account for heat transfer from all directions essential for capturing natural convection and radiation heat transfer, which can vary significantly with spatial positioning, and (3) it is essential for analyzing the fluid flow pathways. This includes understanding the velocity distribution and pressure variations within the system. Accurate fluid flow analysis is critical for assessing heat transfer rates and efficiency.

The main objective of this paper is to propose a three-dimensional mathematical model of the domain and investigate the performance of PV module integrated with finned PCM system by numerical simulation at

different inclinations (θ), number of fins and fin lengths. Rectangular-shaped straight fins are considered in the system. The influence of the number of fins (n) and the inclination angle is also examined. Simulation results are then compared with that of the only system. An optimum finned PV-PCM system is then proposed based on maximum temperature reduction, efficiency enhancement and maximum power output. The effect of fin length on the PV temperature, electrical efficiency, PV electrical output, melting time and convection velocity magnitude is also investigated. While increasing the number of fins, the thickness of the fin is so adjusted that the mass of PCM is kept constant for all the finned PV-PCM configurations. In all, five finned PV-PCM systems are considered with the number of fins (n) = 0 (no fin), 2, 4, 6 and 8, with three different fin lengths at four different inclination angles θ = 0°, 15°, 30°, and 45°. So a total of 60 finned PV-PCM geometries are considered for the present work. The reliability of the model is authenticated by using validation with the available and established experimental data.

METHODOLOGY

Physical Model

The three-dimensional representation of the physical geometry of the finned PV-PCM system on which the present investigations are carried out is shown in Fig. 1. The system consists of a PCM-based heat sink within the aluminium plates, which is mounted on the bottom side of the polycrystalline PV module. Table 1 represents the geometry and properties of different layers of PV module. The PCM used in the system is RT25HC, which is commercially available, and its thermophysical properties are specified in Table 2. The ambient temperature is kept constant at 20 °C; therefore, selecting RT25HC with a melting point of 26.6 °C as PCM is appropriate. The system's inclination (θ) is the angle it makes with the horizontal plane. The depth of the PCM layer is taken as 20 mm. The top surface of the PV module is subjected to incident solar radiation. The top and bottom surfaces are exposed to a combined convective-radiative environment.

Internal longitudinal parallel aluminium fins are provided inside the PCM domain of the system. Different physical configurations of the finned PV-PCM system are established with different lengths and numbers of fins. Different lengths of the fins considered are δ, $3\delta/4$ and $\delta/2$, where δ is the depth of the PCM in the system, which is normal to the plane of the PV module. The thickness of the fin is so varied in such a way that whatever the number of fins in the system, the volume of the fin remains constant. This is achieved by reducing the fin thickness as the number of fins increases. The thickness of the fin and spacing between the fins for different finned PV-PCM systems are shown in Table 3. Every physical configuration of the system will be operated at different tilt angles.

Different operational configurations of the system are established with the variation of the fin arrangement in the system as well as variation of the inclination angle of the system, and this leads to simulating the performance of different configurations of the system and to investigate the effect of fins and inclination of the system on the performance of PV module.
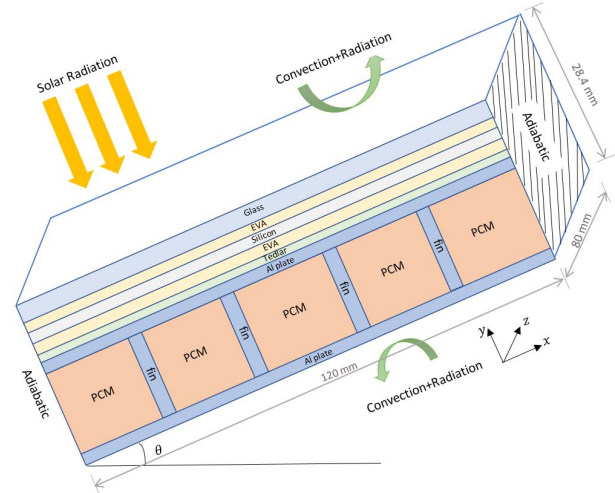

Figure 1. Schematic diagram of three-dimensional finned PV-PCM system.

Table 1. Properties and geometry of PV materials and aluminium (Khanna et al., 2019)

Layer	Thickness (m)	ρ (kg/m^3)	k (W/m.K)	c_p (J/kg K)
Glass	0.003	3000	1.8	500
EVA	0.0005	960	0.35	2080
Silicon	0.0003	2330	147	678
Tedlar	0.0001	1200	0.2	1250
Aluminium	0.002	2675	211	903

Table 2. Properties of RT25HC (Khanna et al., 2018)

Thickness (mm)	20
ρ (kg/m^3)	785/749
k (W/m.K)	0.19/0.18
c_p (J/kg K)	1800/2400
L_h (kJ/kg)	232
μ (Pa s)	0.001798
T_m (°C)	26.6

Table 3. Details of finned structure with varying number of fins

Number of fins	Fin thickness (mm)	Fin spacing (mm)
2	4	40
4	2	24
6	1.33	20
8	1	15

Governing Differential Equations

Governing differential equations of the problem domain and applicable boundary and initial conditions need to be specified to define the problem. Specifying

the governing differential equations leads to modelling the system mathematically. The assumptions used for the mathematical modelling of the system are:

- Incoming solar flux on the PV module is uniformly distributed at an instant.
- Materials of different layers of PV module are considered homogeneous and isotropic.
- Flow of the PCM is considered as Newtonian, laminar, incompressible and unsteady.
- Effect of viscous dissipation is neglected.
- Thermal contact resistances between different layers of the system are neglected.
- Radiation effect inside PCM is neglected.
- Dust and rain effects are neglected.
- Resistive losses in the PV module are neglected.

The unsteady heat conduction equation is invoked for describing the temperature distribution of different layers of PV module and aluminium plates in the system, and it is (Khanna et al., 2018)

$$\rho c_p \frac{\partial T}{\partial t} = k\left(\frac{\partial^2 T}{\partial x^2} + \frac{\partial^2 T}{\partial y^2} + \frac{\partial^2 T}{\partial z^2}\right) + \dot{Q}_g \tag{1}$$

$\dot{Q}_g$ is the rate of heat generation per unit volume in the silicon layer it is to be considered as zero for aluminium layers since they are not involved with heat generation. It can be expressed as

$$\dot{Q}_g = \left[1 - \eta_{PV}\right](\tau\alpha)\, G_T\, A_{si} / V_{si} \tag{2}$$

where $(\tau\alpha)$ is the effective transmissivity-absorbtivity coefficient, and G_T is the solar irradiation in W/m^2. The efficiency of the solar cell is represented by η_{PV} which is defined as (Kaplani and Kaplanis, 2014)

$$\eta_{PV} = 20\left[1 - 0.005\left(T_{PV} - 25°C\right) + 0.085\ln\left(G_T / 1000\right)\right] \tag{3}$$

Modelling of the PCM was done by a modified specific heat capacity method. The governing equations for the PCM, as a fluid coupled with buoyant volumetric force, can be formulated based on the assumptions as:

continuity: $\quad \dfrac{\partial u}{\partial x} + \dfrac{\partial v}{\partial y} + \dfrac{\partial w}{\partial z} = 0 \tag{4}$

x-momentum:

$$\rho\left(\frac{\partial u}{\partial t} + u\frac{\partial u}{\partial x} + v\frac{\partial u}{\partial y} + w\frac{\partial u}{\partial z}\right) = -\frac{\partial P}{\partial x} +$$
$$\mu\left(\frac{\partial^2 u}{\partial x^2} + \frac{\partial^2 u}{\partial y^2} + \frac{\partial^2 u}{\partial z^2}\right) + \rho g_x \beta\left(T - T_m\right) - A(T)u \tag{5}$$

y-momentum:

$$\rho\left(\frac{\partial v}{\partial t} + u\frac{\partial v}{\partial x} + v\frac{\partial v}{\partial y} + w\frac{\partial v}{\partial z}\right) = -\frac{\partial P}{\partial y} +$$
$$\mu\left(\frac{\partial^2 v}{\partial x^2} + \frac{\partial^2 v}{\partial y^2} + +\frac{\partial^2 w}{\partial z^2}\right) + \rho g_y \beta\left(T - T_m\right) - A(T)v \tag{6}$$

z-momentum:

$$\rho\left(\frac{\partial w}{\partial t} + u\frac{\partial w}{\partial x} + v\frac{\partial w}{\partial y} + w\frac{\partial w}{\partial z}\right) = -\frac{\partial P}{\partial z} +$$
$$\mu\left(\frac{\partial^2 w}{\partial x^2} + \frac{\partial^2 w}{\partial y^2} + +\frac{\partial^2 w}{\partial z^2}\right) + \rho g_z\left(T - T_m\right) - A(T)w \tag{7}$$

thermal energy:

$$\rho c_p \frac{\partial T}{\partial t} = \frac{\partial}{\partial x}\left(k\frac{\partial T}{\partial x} - \rho c_p u T\right) + \frac{\partial}{\partial y}\left(k\frac{\partial T}{\partial y} - \rho c_p v T\right)$$
$$+ \frac{\partial}{\partial z}\left(k\frac{\partial T}{\partial z} - \rho c_p w T\right) \tag{8}$$

For the solid phase of the PCM, the effect of velocity components in Eqn. (8) becomes zero. The third term on the RHS of momentum equations is the buoyant force which is volumetric in nature, and it results in motion in the melted PCM due to variation in density. The secondary volumetric force is represented by the last term in the RHS of momentum equations, and it is included to help the solver to arrive at the PCM velocities equal to 0 in the solid phase quickly. The porosity operator is derived from the Carmen-Kozeny equation for porous media, which is represented by $A(T)$ (Brent et al., 1988), and it is,

$$A(T) = \frac{C_m\left(1 - B(T)\right)^2}{B(T)^3 + \psi} \tag{9}$$

The value of C_m specifies how quickly the velocity is decreased to zero when the PCM is in the solid state, and it is determined by the morphology of the PCM. The value of C_m is generally taken as 10^5 for organic PCM (Khanna et al., 2017). The denominator was added with a very small computational constant ψ to prevent division by zero. In effect, the initial large value of $A(T)$ swamps out all the terms in the governing equations and effectively forces velocity to reach zero in completely solid elements. The validity of the Carman-Kozeny equation in modelling the flow mushy zone was shown experimentally by Poirier (1987).

The viscosity of the PCM can be modified as

$$\mu(T) = \mu_l\left(1 + A(T)\right) \tag{10}$$

It ensures the usage of very high and very low viscosities in the regions of PCM that are below the solidus temperature, $(T_m - \Delta T / 2)$, and above the liquidus temperature $(T_m + \Delta T / 2)$, respectively.

The density and thermal conductivity of the PCM can be modelled as (Khanna et al., 2017)

$$\rho_{pcm}(T) = \rho_s + (\rho_l - \rho_s)B(T) \qquad (11)$$

$$k_{pcm}(T) = k_s + (k_l - k_s)B(T) \qquad (12)$$

where $B(T)$ is the liquid fraction which characterises the phase change, and it can be defined as (Balavinayagam et al., 2021)(Khanna et al., 2017)

$$B(T) =
\begin{cases}
0 & \text{if } T < (T_m - \Delta T/2) \\
(T - T_m + \Delta T)/(2\Delta T) & \text{if } (T_m - \Delta T/2) \le T \le (T_m + \Delta T/2) \\
1 & \text{if } T > (T_m + \Delta T/2)
\end{cases} \qquad (13)$$

The modified specific heat capacity of the PCM is (Unnikrishnan et al., 2023)

$$c_{p,pcm}(T) = c_{ps} + (c_{pl} - c_{ps})B(T) + L_h D(T) \qquad (14)$$

and

$$D(T) = \frac{e^{\frac{-(T-T_m)^2}{(\Delta T/4)^2}}}{\sqrt{\pi(\Delta T/4)^2}} \qquad (15)$$

where $D(T)$ is a smoothed Dirac delta function, with a value of zero everywhere except in the transition zone of the PCM. This function is used to disperse PCM's latent heat evenly around the melting temperature in the transition region.

Boundary and Initial Conditions

The top and bottom surfaces of the system are subjected to combined convection and radiation heat transfer. A solar irradiation G_T is uniformly applied on the front surface of the PV module as input.

The boundary condition on the top surface of the system is:

$$k_g\left(\frac{\partial T}{\partial y}\right) = \left(h_{free} + h_{forced}\right)\left(T_{amb} - T_g\right) + \alpha_g G_T + \varepsilon_g \sigma\left(T_{amb}^4 - T_g^4\right) \qquad (16)$$

The boundary condition on the bottom surface of the system is:

$$k_{al}\left(\frac{\partial T}{\partial y}\right) = \left(h_{free} + h_{forced}\right)\left(T_{al} - T_{amb}\right) + \varepsilon_{al} \sigma\left(T_{al}^4 - T_{amb}^4\right) \qquad (17)$$

where h_{free} and h_{forced} are the free and forced convection heat transfer coefficients, respectively,

which are defined as (Kaplani and Kaplanis, 2014; Khanna et al., 2017)

$$h_{free} =
\begin{cases}
\dfrac{k_a}{L_c}\left[0.68 + \dfrac{0.67\left(Ra_L \sin\theta\right)^{0.25}}{\left(1 + \left(\dfrac{0.492 k_a}{\mu c_p}\right)^{9/16}\right)^{4/9}}\right] & \text{if } Ra_L \le 10^9 \\[3em]
\dfrac{k_a}{L_c}\left[\left(0.825 + \dfrac{0.387\left(Ra_L \sin\theta\right)^{1/6}}{\left(1 + \left(\dfrac{0.492 k_a}{\mu c_p}\right)^{9/16}\right)^{8/27}}\right)^2\right] & \text{if } Ra_L > 10^9
\end{cases}$$

$$(18)$$

where Ra_L is the Rayleigh number, which is defined as (Incropera and Dewitt, 1985)

$$Ra_L = \frac{g\left(1/T_f\right)\left(T - T_a\right)L_c^3}{\nu\,\alpha} \qquad (19)$$

with α and ν as thermal and momentum diffusivities of air, respectively, at the film temperature (Fujii and Imura, 1972).

$$h_{forced} =
\begin{cases}
\dfrac{2k\left(0.332 Re_L^{\frac{1}{2}} Pr^{\frac{1}{3}}\right)}{L_c} & \text{if } Re_L \le 5\times10^5 \\[2em]
\dfrac{2k Pr^{\frac{1}{3}}\left(0.037 Re_L^{0.8} - 871\right)}{L_c} & \text{if } Re_L > 5\times10^5
\end{cases} \qquad (20)$$

with Re_L and L_c as Reynolds number and characteristic length, respectively.

The side walls of the system are insulated, and hence, the boundary conditions at the side walls are:

$$\left(\frac{\partial T}{\partial x}\right) = 0 \qquad (21)$$

front and rear side walls: $\left(\dfrac{\partial T}{\partial z}\right) = 0 \qquad (22)$

No slip condition at six boundary surfaces of the PCM in the system leads to the boundary condition at all the surfaces.

$$u = v = w = 0 \qquad (23)$$

At all the interfaces in the system, the boundary condition is applicable, and it can be defined as

$$k_r \left(\frac{\partial T_r}{\partial y} \right) = k_s \left(\frac{\partial T_s}{\partial y} \right) \qquad (24)$$

where r and s represent the materials of two different layers on either side of the interface in the system.

Initial Conditions:

$$At\ t = 0,\ u\ =\ v\ =\ w\ =\ 0 \qquad (25)$$

$$At\ t = 0,\ T = T_i = 20\ °C \qquad (26)$$

The value of G and other inputs required to carry out the simulation are specified in Table. 4.

Table 4. Inputs to simulation

Parameter	Value
PCM thickness (mm)	20
β (K^{-1})	9.1×10^{-4}
T_a (°C)	20
G_T (W/m^2)	1000
$(\tau\alpha)$	0.9
ΔT (°C)	2

NUMERICAL PROCEDURE and VALIDATION of THE MODEL

The simulation of all the configurations of the system considered in the present work is carried out using COMSOL *Multiphysics* 6.0. Easy linking and solution of partial differential equations related to different fields of physics are possible by the COMSOL *Multiphysics* software based on the finite element approach. The coupled problem of heat transfer and fluid flow (laminar) in melted PCM is modelled using continuity, momentum equations with Boussinesq approximation and energy equations by employing the conservation principles and solved using COMSOL software. The three-dimensional geometry of the PV-PCM system is developed using the geometry module of the COMSOL interface, and appropriate materials with dimensions and thermophysical properties are attached to each PV-PCM layer and fins. Different configurations of PV-PCM system geometries considered in the present work are established, and the same is shown in Fig. 2 when they are operating at 15° inclination. Aspects of physics involved in the development of the present mathematical model are heat transfer in solids (PV, solid PCM fins and aluminium), heat transfer in fluids (liquid PCM) and laminar fluid flow (liquid PCM), which replicate heat transfer and buoyancy-driven fluid flow along with phase transition. Material properties of the PCM and variables and functions involved in the mathematical model of the PCM are defined to establish the PCM domain in the PV-PCM system.

The COMSOL Multiphysics® provides an automated process of meshing the geometry of the model. The default physics-controlled mesh sequence setting is invoked for the meshing of the field's geometry. The physics-controlled meshing process examines the

physics to determine the size attributes and operations needed to create a mesh that is suited to the task. The tetrahedral mesh is used in the three-dimensional domain of the present system. Under the physics-controlled mesh sequence type, the different mesh settings from *coarse* to *extra fine* are chosen for conducting grid independence study, as shown in Fig. 3. The study shows that going from *fine* to *extra fine* yields no significant change in the PV temperature, therefore, *fine* mesh is selected as the preferred mesh option. There are 176822 domain elements, 45698 boundary elements, and 2308 edge elements in the final mesh. Fig. 4 shows the mesh that was created for the system with eight fins at 30° inclination.

Figure 2. PV-PCM system configurations with different numbers of fins at 15° inclination.
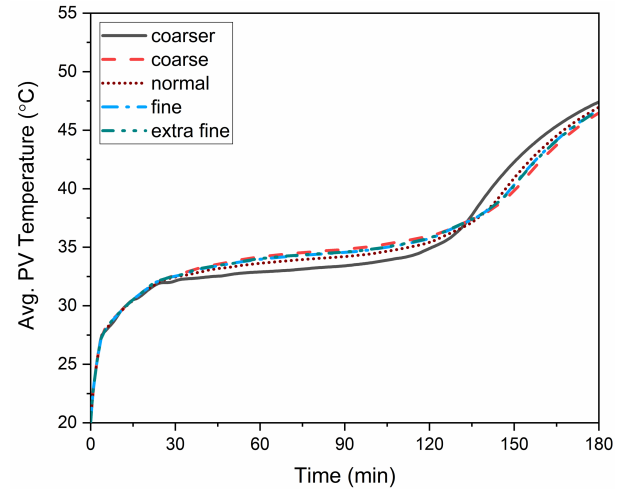

Figure 3. Grid Independence study.

Most time-dependent problems like the current one in COMSOL *Multiphysics* are solved by default using an adaptive time-stepping technique. The solver will adjust the appropriate time-step size to maintain the chosen *Relative Tolerance* of 0.001. Lowering the relative tolerance to smaller values results in smaller time steps, thereby improving solution accuracy and reducing solving time. Here, the initial time-step size is set to 0.001 sec, and the maximum time step that can be taken is set to one second. The solver will automatically adjust the time-step size as needed to address any fast variations in the solution during the solution procedure. The implicit Backward Differentiation Formula (*BDF*) with an order of accuracy equal to 2 is utilised as the time-stepping approach.

Figure 4. Generated mesh.

The current model is validated by comparing the simulation predictions with the experimental results of Huang et al. (2011) for the thermal performance of a PV-PCM system with internal fins. The fins are provided in the PCM domain with 24 mm spacing, and the top surface of the PV-PCM system is exposed to a constant flux of 750 W/m^2 with an initial temperature of 19°C. RT27 is used PCM in the system for validation purpose. The measurements of the PV-PCM system are 0.132 m × 0.04 m × 0.3 m. The experimental average temperature of the finned PV-PCM system is compared with the simulated values, as shown in Fig. 5. It can be inferred from the comparison that the simulated predictions are found to be in
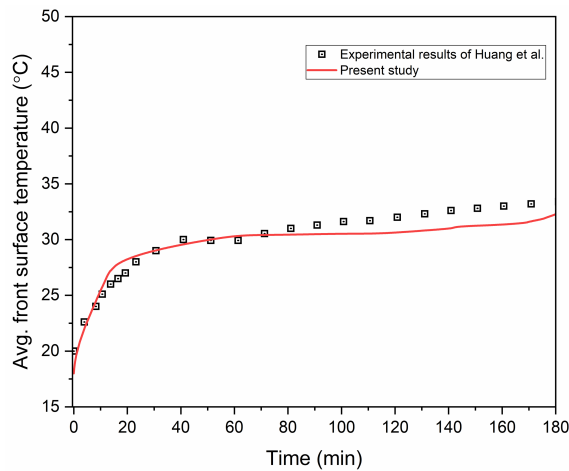
reasonable agreement with the experimental results.

Figure 5. Validation of the model.

SIMULATION OF THE SYSTEM

The performance of PV module in different configurations of PV-only systems, PV-PCM systems (no fins) and finned PV-PCM systems considered in the present work are numerically simulated. The effect of including the PCM and fins in the system on the performance of the PV module was analysed by comparing it with the performance of the only system at different inclinations. The numbers of fins considered for the study are no fin, 2, 4, 6 and 8, and different inclinations of the system considered are 0°, 15°, 30 and 45°. All the configurations of the system systems under the study are subjected to constant solar radiation flux throughout the duration of the

simulation, considered with an ambient temperature. The area of the PV module is 120 mm×60 mm. Fins having lengths of 10 mm (half fin), 15 mm (three-quarter fin) and 20 mm (full fin) are considered in the PCM in different systems. The average PV temperature profiles, temperature contours, and PV efficiency variation are simulated for all the PV-PCM and finned PV-PCM systems and compared with the conventional PV-only system. The time-dependent study is carried out for all the configurations.

RESULTS AND DISCUSSION

The investigations were carried out for different configurations of finned PV-PCM systems with the inclusion of longitudinal fin with multiple numbers of fins and lengths at various inclinations, and the effect of fins and PCM on the performance of the PV module was explored.

For PV-only Case

Fig. 6 depicts the temporal evolution of average PV temperature and PV efficiency of standard PV alone systems at various orientations. The temperature rises rapidly with time, reaching an almost steady-state temperature of 88.7 °C and 65.4 °C for 0° and 45° inclinations, respectively, in almost 45 min, as shown in Fig. 6 (a). External natural and forced convection, along with radiation, are the sources of cooling. The PV temperature decreases because of the increased external natural convection heat transfer rate with an inclination angle. The lowest PV temperature is observed for the system with a 45° inclination. The efficiency of the PV module follows the opposite trend compared to PV temperature, and PV efficiency rises as the inclination rises, as shown in Fig. 6 (b).

For Finned PV-PCM

Fig. 7 shows the time-dependent variation of average PV temperature of all PV-PCM system (no fin) configurations and finned PV-PCM system configurations with different fin lengths of 10 mm, 15 mm and 20 mm at different inclinations. The average PV temperature decreases with the increasing inclination of the system, with the lowest PV temperature recorded at an inclination of 45°. When the PV-PCM system is in horizontal orientation (θ = 0°), the presence of the buoyant forces is negligible, and convection currents within the melted PCM of the system hardly exist. As a result, conduction is the primary mode of heat transfer within the PCM, resulting in thermal stratification. Due to this, the rate of heat transfer involved through PCM is less, which leads to the maximum PV temperature for horizontal systems than systems at other inclinations. There is a significant presence of buoyant force, which is volumetric in nature and thus, the existence of convection currents in the melted PCM for sloped PV-PCM systems. Convection heat transfer becomes the major heat transfer mode within the melted PCM due

to this increased intensity of buoyant volumetric force. So, natural convection heat transfer plays a vital role, which affects the melting rate of PCM. The direction of the gravitational force vector is highly important in this scenario. The intensity of the convection heat transfer rate so developed increases with increasing inclination, thereby enhancing the rate of heat transfer from the PV module and lowering the temperature of the module. Hence, it is critical to look into how the inclination of the overall system affects the thermal processes that occur within it.

It is evident for PV-PCM systems from Fig. 7 that the solid PCM first receives heat, resulting in a sharp increase in time-dependent temperature initially due to sensible heating. After that, the melting process of PCM begins and continues until the solid PCM becomes liquid. Within the melting zone, the PCM temperature rises slightly. Whatever heat is transferred from the PV module is used by PCM to satisfy its latent heat requirement for undergoing a phase change. The time interval required from the commencement of the phase change process to its completion is the actual period of thermal regulation. Heat transfer to the PCM after the phase change process leads to sensible heating of the liquid PCM, which causes the steep temperature rise. This behaviour can be observed for all PV-PCM systems irrespective of its inclination.

However, the poor thermal conductivity of paraffin PCMs creates a hurdle for the higher heat extraction from the PV module to the PCM in the system. The heat transfer rate is lower for sensible heating of the solid PCM because as the layer thickness increases, conduction is the only heat transfer mode through the solid PCM at any inclination of the system. The thermal resistance of the PCM is too high for the required phase transformation rate because of its low thermal conductivity. Natural convection can form in the liquid PCM layer due to a temperature difference between the heated boundary and the solid section of the PCM, complicating the physical scenario. The system's geometry and PCM thickness determine the extent of natural convection and its contribution to overall heat transfer. Aluminium Fins were included in the system to overcome the low thermal conductivity of the paraffin PCM in the present work. Low density and high thermal conductivity of aluminium compared to many other metals results in a significantly lighter thermal energy storage device. The inclusion of fins in the PV-PCM system transforms the system into a finned PV-PCM system. Fins of multiple numbers and different heights are used to establish different finned systems. This leads to a considerable reduction of the operating temperature of the PV module in the finned PV-PCM systems with different numbers of fins and fin lengths considered at any inclination compared to the PV-PCM system, as shown in Fig. 7. The presence of fins within the PCM enhances the heat transfer rate from the PV module to PCM and improves the module's performance in the finned PV-PCM systems at all inclinations. A steep increase in temperature of the module during sensible heating of the PCM in the solid and liquid phases and a slight increase in temperature of the module during the phase change process of the PCM are also seen in all the configurations of the finned PV-PCM systems. It is worth noting that the temperature trends converge in the end, indicating that the entire PCM has melted. The presence of fins accelerates all the thermal processes, and the thermal regulation happens at a lower temperature compared to the unfinned cases.

The fin heights of 10 mm, 15 mm and 20 mm are selected and distributed evenly over the PCM domain. Fins are used in PCM to increase the heat transfer surface area. The liquid PCM will have more thermal contact with the heat transfer surface when fins are introduced into the system, and thermal resistance to heat transfer will be lowered consequently. The heat transfer rate from PV to PCM and inside the PCM is greatly improved by the presence of fins because more area is accessible for heat transfer. As a result, the PV temperature drops, increasing its energy conversion performance.
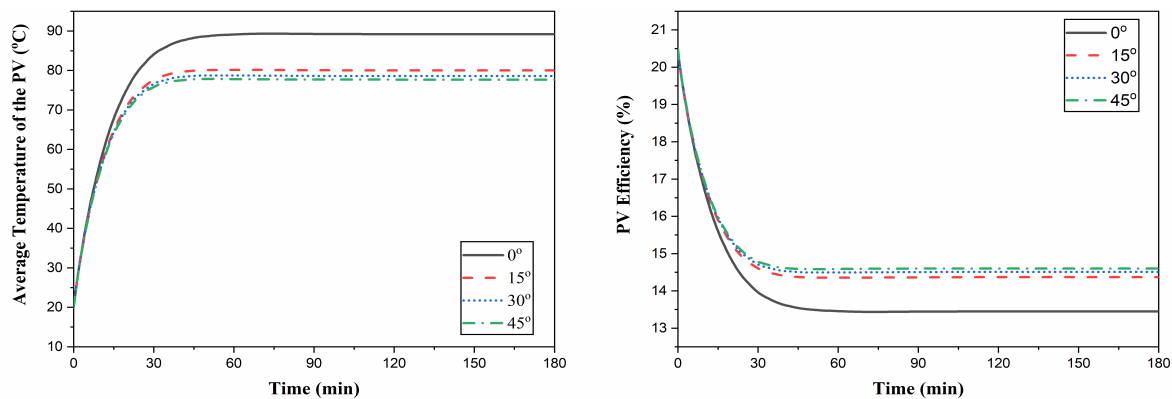

Figure 6. Variations of (a) average PV temperature and (b) PV efficiency with time for different inclinations of PV-only system.

From Fig. 7, it is evident that for the systems with fin lengths of 10 mm and 15 mm, the temperature is lowest initially for finned PV-PCM system with 8 fins up to 50 min for 10 mm fin systems and 80 min for 15 mm fin systems and then, the system with 6 fins shows the lowest temperature for all the angles except for the system with 10 mm fins at 0° case. The system with 2 fins shows the lowest average PV temperature after 50 min at 0° inclination with 10 mm fins. For the 20 mm fin length case (full fin), the lowest average PV temperature is obtained for the finned PV-PCM system

with 6 fins for all the angles. When comparing different lengths of fins, systems with 20 mm fin lengths are found to be better systems with the lowest PV temperature. It is also clear that the relative temperature decreases with an increase in the inclinations of the systems. Considering the fin lengths, the number of fins and inclinations, the optimum system, i.e., one with the lowest PV temperature, is found for the PV-PCM PCM system with 6 fins at an inclination angle of 45°.
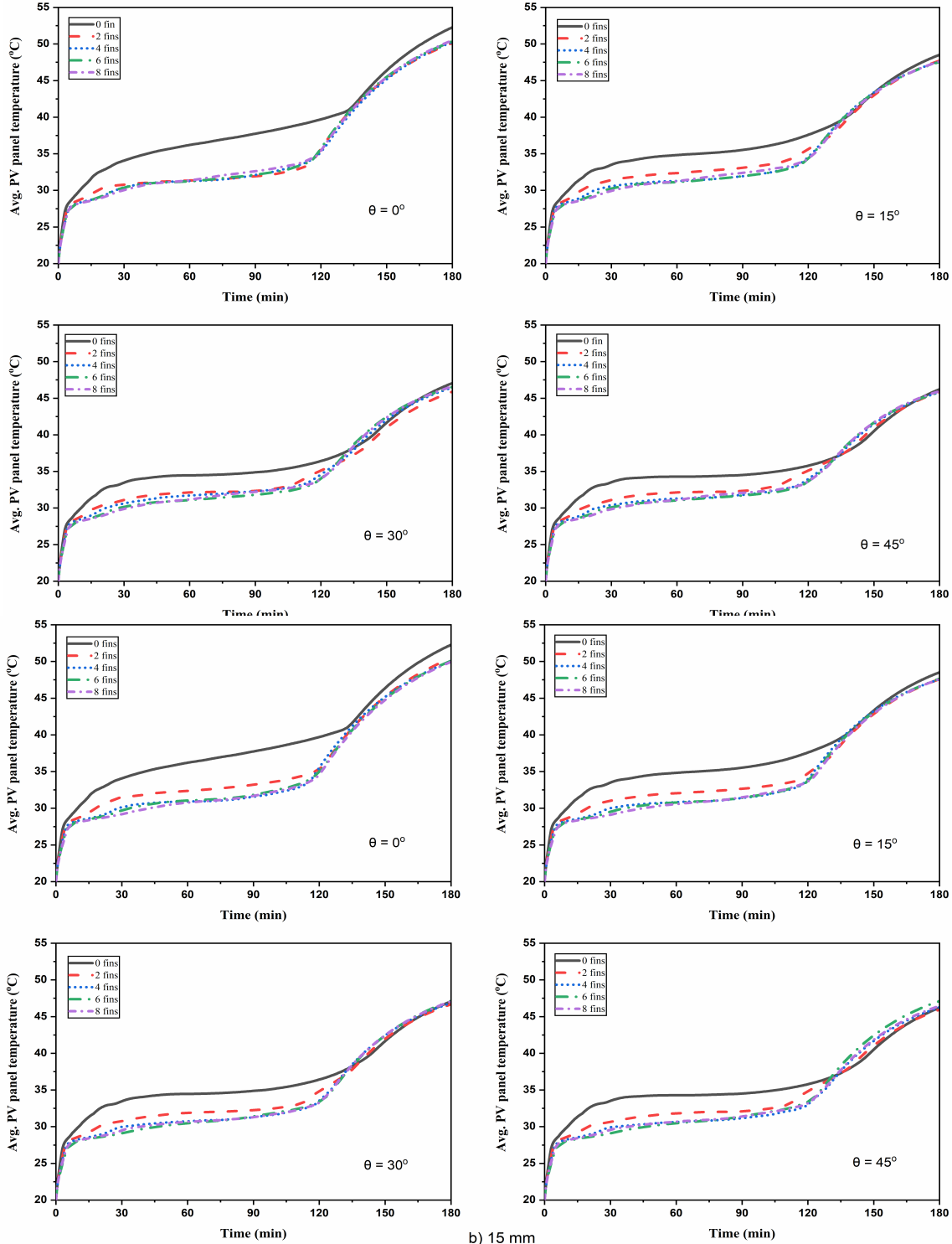
b) 15 mm
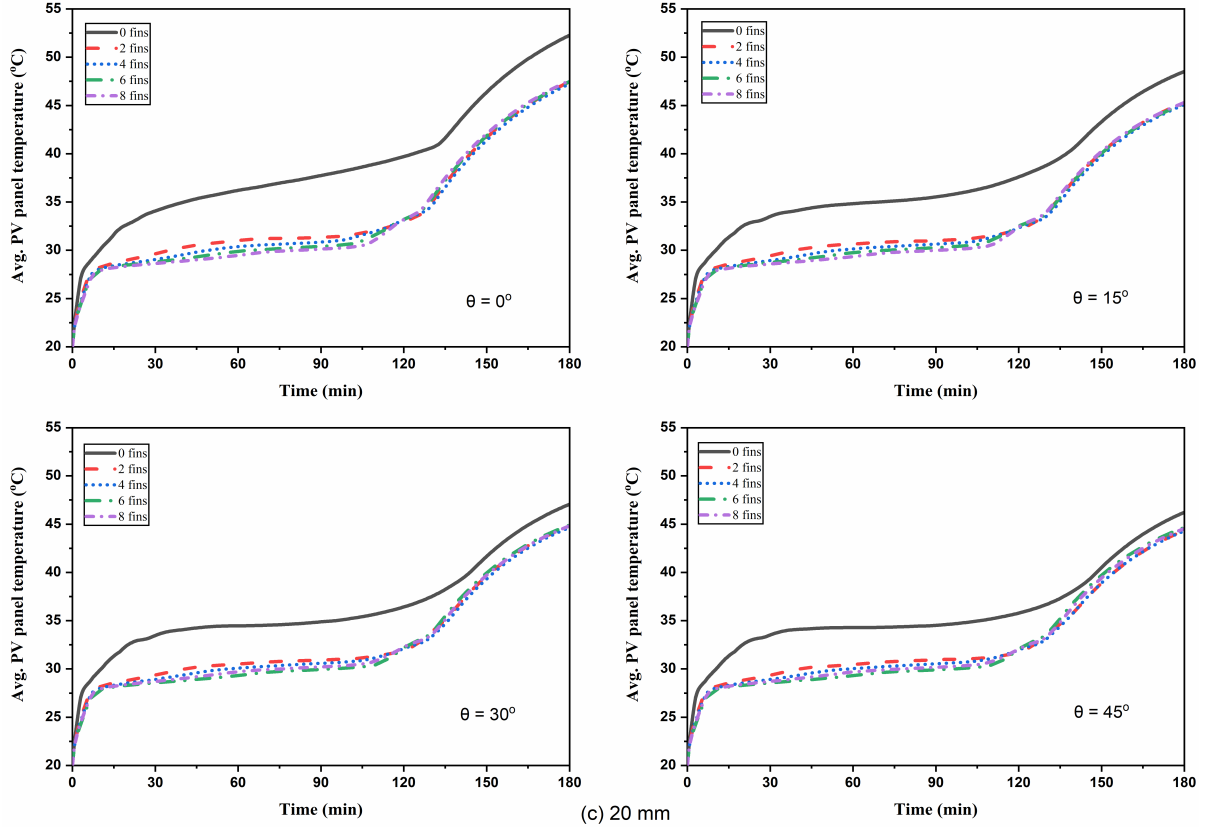
Figure 7. Variation of the mean temperature of the module with time for PV-PCM and finned PV-PCM systems with fin lengths (a) 10 mm, (b) 15 mm and (c) 20 mm at different inclinations.

The temperature contours of PV-PCM system (no fin) and finned PV-PCM (fin length of 20 mm) systems with the number of fins of 2, 4, 6 and 8 for the inclinations of 0°, 15°, 30°, and 45° at different instants are shown in Fig. 8 (a) - (e). The figures indicate that the temperature front for the horizontal system with the inclination of 0° orientation travels uniformly downwards with the progress of time for PV-PCM and finned PV-PCM systems. In the presence of fins for finned PV-PCM systems, the temperature front travels faster compared to the PV-PCM system due to the enhanced heat transfer rate to the PCM. The temperature front movement in inclined systems is non-uniform due to the presence of a buoyancy effect within the melted PCM. As solar radiation falls on the PV panel's front surface, the temperature rises, and heat transfer from the PV panel to the PCM begins. In its solid phase, the PCM absorbs and stores energy in the form of sensible heat as its temperature rises.

Storage of energy in the form of latent heat in PCM commences when the temperature of a solid PCM approaches the transition temperature. The temperature profile in inclined systems is non-uniform because of the existence of melted PCM's buoyancy effect by virtue of convection currents present in it. At first, pure conduction dominates the heat transfer process in PCM. The temperature front remains about parallel during the initial conduction-dominated melting process. As time

progresses in the interaction between the module and PCM, the temperature front moves closer to the bottom. With time, the motion of the liquid PCM will be detected in the upper right portion of the melt zone, followed by a nearly immobile liquid PCM below it. Both conduction and convection heat transfer modes dominate the melting process in such a transition state. In the upper portion of the PCM liquid zone (dominated by convection), the temperature profile curves sharply, followed by a front parallel to the left wall in the lower half of the liquid region (conduction-dominated). The height of the convection-dominated zone increases with time throughout the transition phase. The convection-dominated zone of the transition regime will fill the whole domain of the PCM. The spontaneous circulation of liquid PCM distinguishes this regime. At a certain point in time, the upper part of the curved melting front makes contact with the right vertical wall. In the liquid phase, convection is the predominant route of heat transfer, while in the solid phase, conduction is the primary mode of heat transfer. After completing the melting process, the melted PCM absorbs energy from the PV module in sensible heat, and its temperature rises. During sensible heating, the heated liquid PCM near the upper aluminium plate flows downwards and circulates throughout the container. The inclusion of fins reduces PV temperature significantly, as shown by the contour plots, by virtue of improved heat transfer rate from the module to PCM in the system.
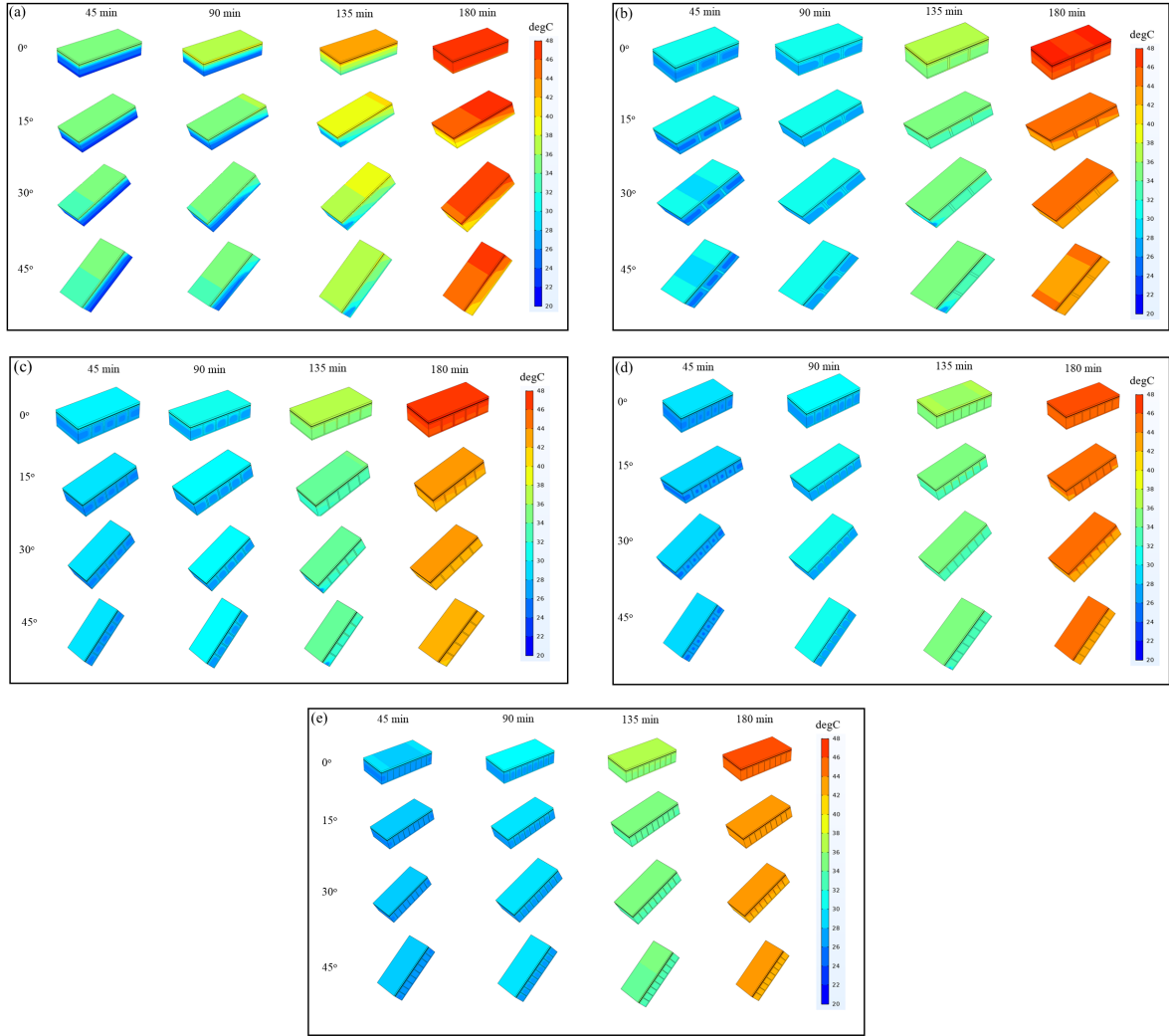
Figure 8. Temperature profiles and liquid PCM movement at various inclinations in different systems: (a) No fin (PV-PCM), (b) 2 fin, (c) 4 fin, (d) 6 fin and (e) 8 fin at different instants.

The trend of efficiency of the PV module is opposite to its temperature, and the same is explained with Eqn. (3). For mono and polycrystalline PV cells, an increase in operating temperature causes a decrease in open-circuit voltage, fill factor and power output, with an increase in short circuit current, which ultimately results in the loss of electrical efficiency of the module and irreversible damage to the PV cell materials. PV module works better at lower temperatures, as shown in Fig. 9. (a)-(c) At the system's inclinations, 45° and 0°, the highest and lowest efficiency trends are reported, respectively, for PV-PCM and finned PV-PCM systems of fin lengths 10 mm, 15 mm and 20 mm. The efficiency of the PV module is highest at 45° inclination for the finned PV-PCM system with 6 fins, as the PV temperature is lowest for this case.
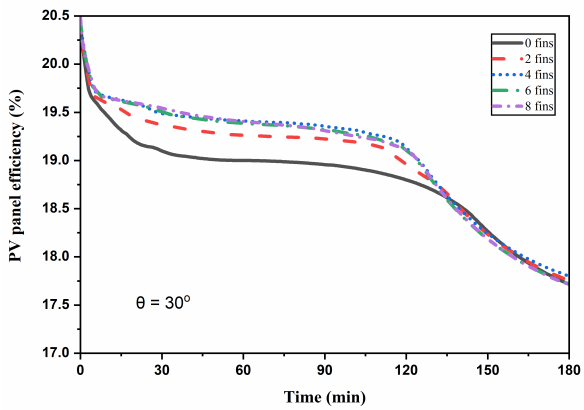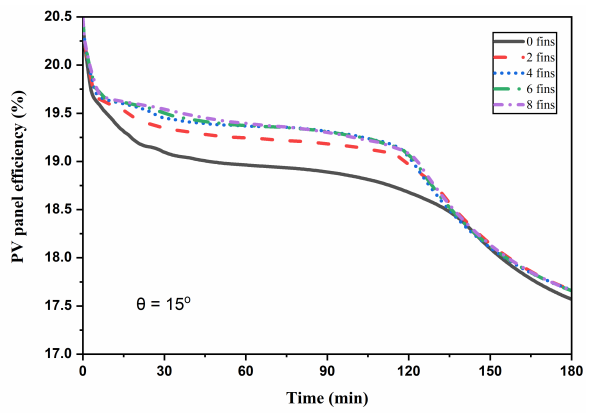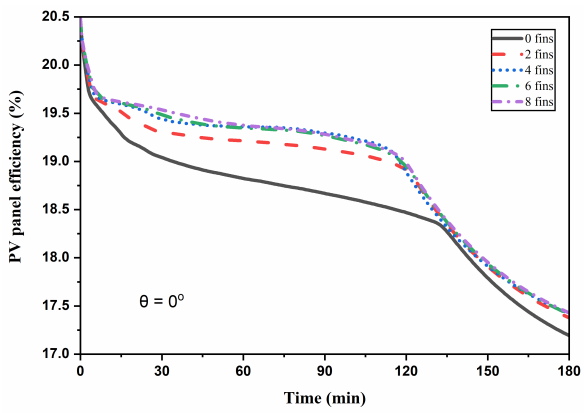
Trends of mean PV temperature and electrical efficiency of PV-PCM systems without any fins are compared with corresponding PV-only systems for each system's inclination. The maximum reduction in mean temperature and enhancement in the electrical efficiency of the module in the PV-PCM system over PV only system at each inclination is shown in Fig. 10.

The maximum PV temperature reduction of 53.4 °C, 45.58 °C, 44.4 °C, and 43.63 °C are achieved with PV-PCM systems at inclinations of 0°, 15°, 30°, and 45°, respectively. Maximum and minimum relative enhancement in electrical efficiency is obtained as 39.6% and 30.45% for PV-PCM systems at the inclinations of 0° and 45°, respectively.

Trends of mean PV temperature and electrical efficiency of PV-PCM systems without any fins are compared with corresponding PV-only systems for each system's inclination. The maximum reduction in mean temperature and enhancement in the electrical efficiency of the module in the PV-PCM system over PV only system at each inclination is shown in Fig. 10. The maximum PV temperature reduction of 53.4 °C, 45.58 °C, 44.4 °C, and 43.63 °C are achieved with PV-PCM systems at inclinations of 0°, 15°, 30°, and 45°, respectively. Maximum and minimum relative enhancement in electrical efficiency is obtained as 39.6% and 30.45% for PV-PCM systems at the inclinations of 0° and 45°, respectively.
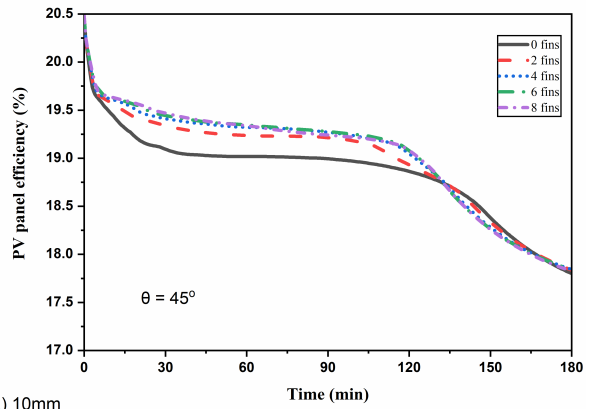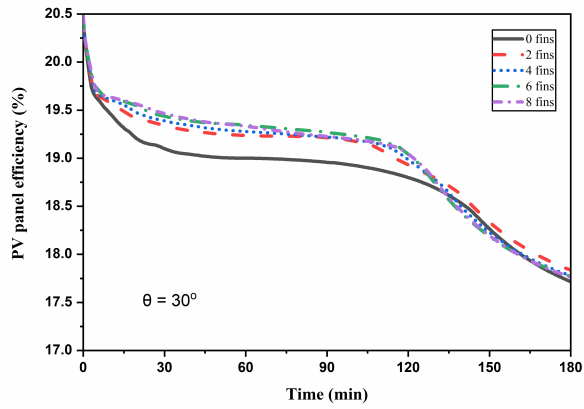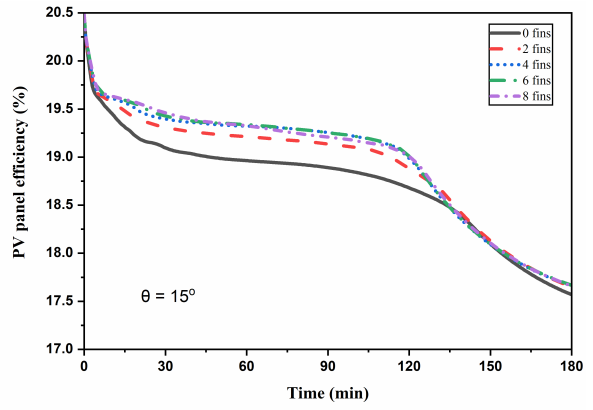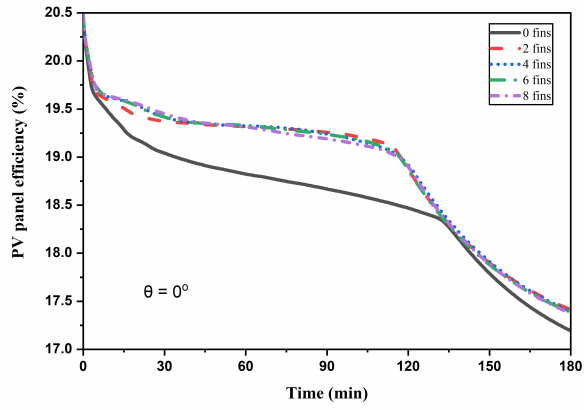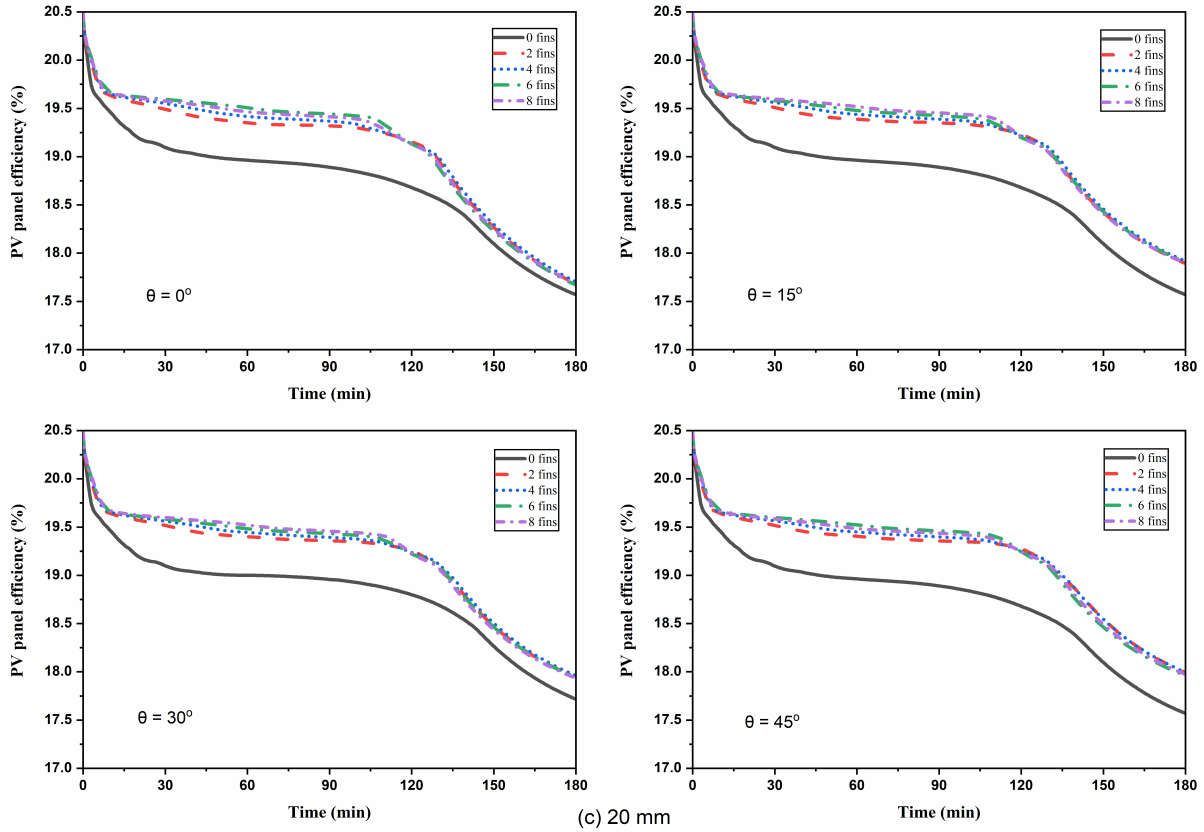
a) 10mm

b) 15 mm

Figure 9. Variation of electrical efficiency of the module with time for PV-PCM and finned PV-PCM systems with fin lengths (a) 10 mm (b) 15 mm and (c) 20 mm at different inclinations.
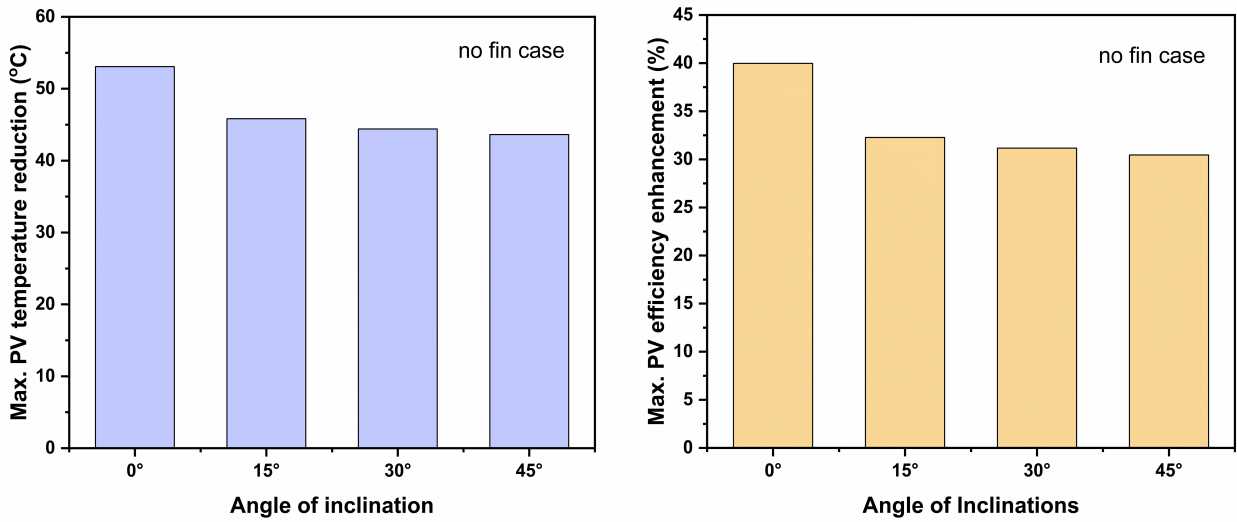

Figure. 10 Comparison of (a) maximum reduction in PV temperature and (b) Maximum percentage increase in efficiency of PV-PCM systems of different orientations with PV-only cases.

Fig. 11 shows the highest PV temperature reduction for finned PV-PCM systems with different fin lengths and the number of fins at various orientations compared to the PV-only system. The inclusion of fins leads to the best results in the form of the highest temperature reduction of the module for horizontal systems due to the involvement of conduction heat transfer from the module to PCM in such systems. For horizontal systems, the conduction heat transfer rate is enhanced due to the inclusion of fins without any effect that reduces the rate of heat transfer. However, in the inclined systems, convection heat transfer mode is present when the PCM is in the liquid phase. Increased heat transfer area with the inclusion of the fins leads to a higher rate of heat transfer in inclined systems. But, higher surface area with finned systems will also enhance the fluid friction, which reduces the strength of convection currents. Hence, in the inclined systems, two competing opposite effects in the form of increased heat transfer rate and fluid friction are present, leading to a relatively lower effect compared to horizontal systems. As the figure indicates, for any inclination, with the

increase in fin length, the PV module temperature is further reduced, and consequently, electrical efficiency is improved. So when comparing the different fin lengths, systems with 20 mm fin length give the best results in terms of maximum PV temperature reduction and improving PV efficiency. Among the systems with 20 mm fin length, the performance statistics are relatively best when number of fins equals 6. It is also apparent that the effect of the inclusion of fins is greatest for horizontal systems with an inclination of 0° and diminishes as the inclination angle increases. The highest temperature reduction of 59.65 °C is observed for the PV-PCM system with 6 fins for fin length = 20 mm at an inclination angle 0°, and the lowest is observed for the system with 2 fins for 10 mm fin length at an inclination angle of 45°.
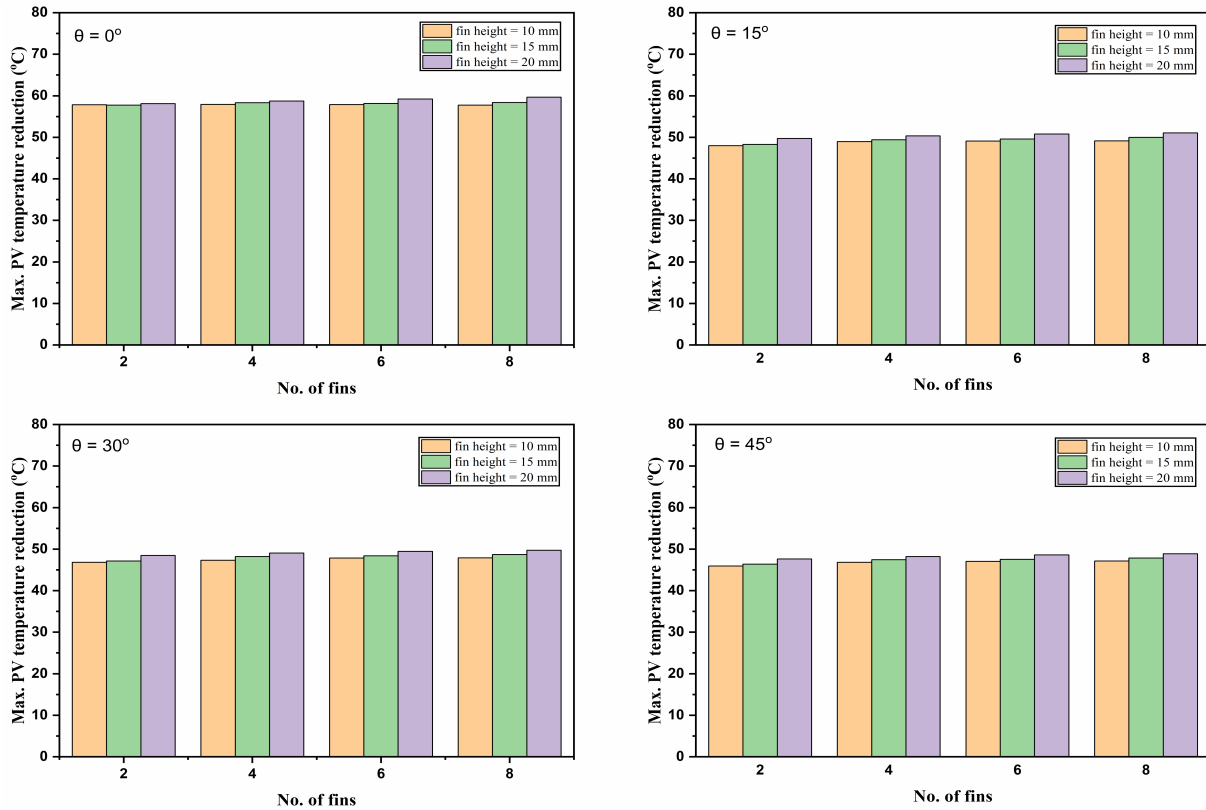

Figure 11. Comparison of maximum temperature reduction of finned PV-PCM with respect to multiple numbers of fins and inclinations for different fin lengths.

The comparison of maximum enhancement in electrical efficiency of the module for finned PV-PCM systems with different fin lengths and number of fins at various inclinations with PV-only systems is shown in Fig. 12. It is clear that efficiency levels increase with the increase in fin lengths, with a maximum obtained for 20 mm fin length (full length) configuration for a particular number of fins and inclination. The highest and lowest enhancement values of efficiency are obtained for systems with 0° and 45° orientations, respectively, indicating that the effect of fin inclusion is more prominent when the inclination is low. Maximum efficiency enhancement of 45.08% is obtained for the system with 6 fins at inclination 0° for fin length 20 mm and the least value of 32.07% obtained for 10 mm 2 finned PV-PCM systems at 45°. It is clear that the inclusion of fin is most effective when the inclination of the system is small.

As the PV efficiency values are highest for 20 mm fin length systems, the comparison of the maximum power output of PV module for different finned PV-PCM systems with fin lengths of 20 mm, including the unfinned system at different inclinations are shown in Fig. 13. There is a marked improvement in PV module power output for finned systems compared to unfinned one. The PV output levels increase with the increase in inclination angle for a particular number of fins. The PV power output is found to increase with the increase in number of fins for finned PV-PCM systems up to 6 fins, then decreases for the system with 8 fins. The maximum power output of 14.16 W is observed for the PV-PCM system with 6 fins at an inclination angle of 45°.

The time taken for the complete melting of PCM with respect to inclinations for different numbers of fins with 20 mm fin length is shown in Fig. 14. The figure shows that the melting is slower for unfinned systems compared to finned ones, indicating a lesser heat transfer rate inside PCM of unfinned systems. There is a considerable decrease in melting time with an increase in inclination as the heat transfer rate is higher to PCM in the systems at higher inclinations. This is due to the increased natural convection heat transfer rate within the melted PCM due to the existence of a

higher buoyant force. The reduction of PCM melting time with the increase in number of fins is because when the number of fins is higher, the surface area available for heat transfer within PCM is also higher.

The lowest melting time of PCM is obtained as 132 min for the system with 8 fins with an orientation of 45°, and the highest melting time is 148.7 min for the unfinned system with $\theta = 0$.
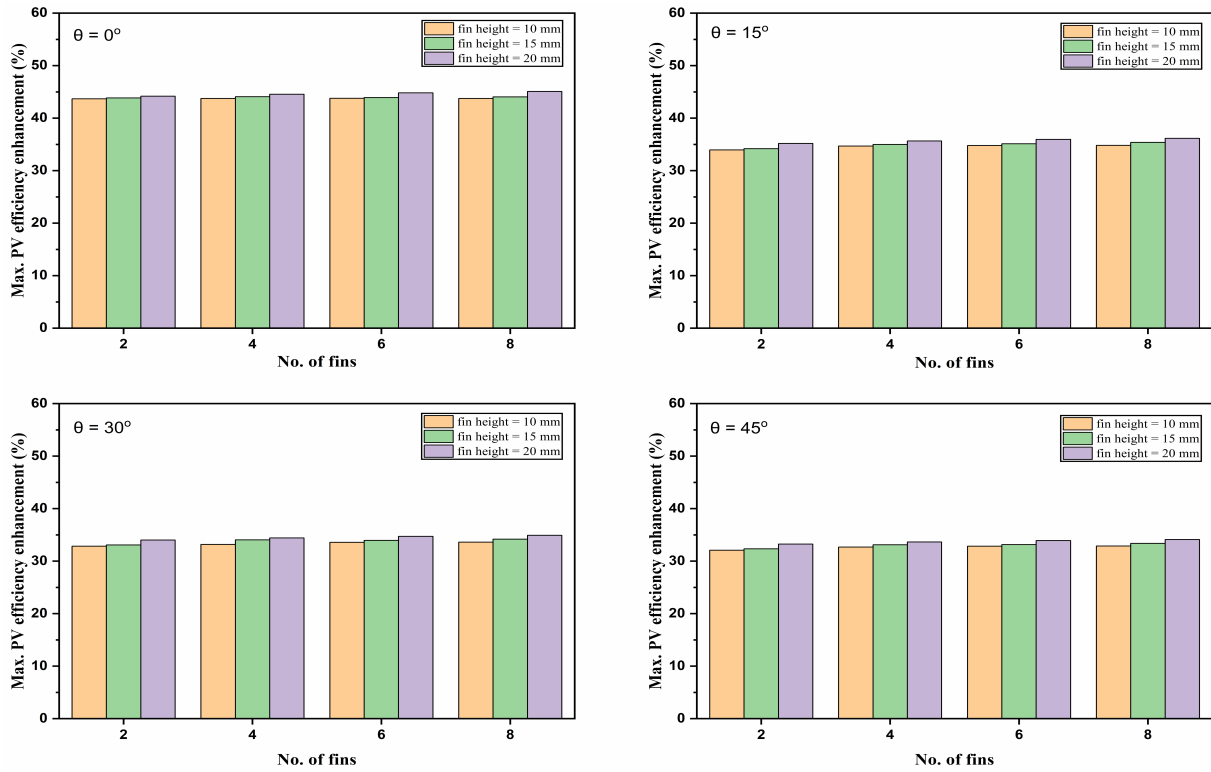

Figure 12. Comparison of maximum efficiency enhancement of finned PV-PCM systems with respect to multiple numbers of fins and fin lengths for different inclinations.

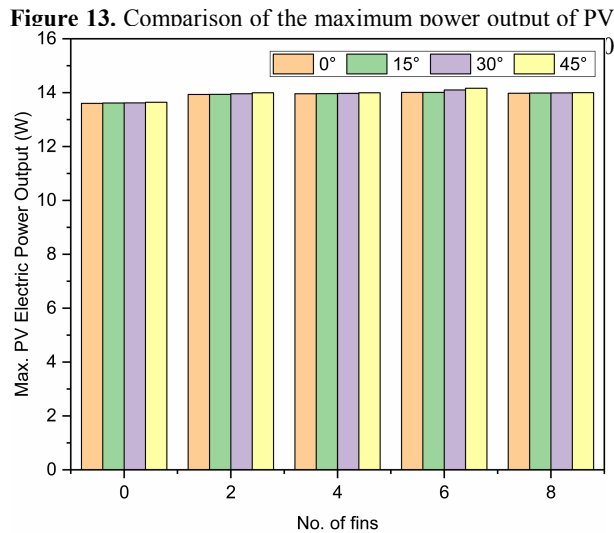**Figure 13.** Comparison of the maximum power output of PV

Fig. 15 (a)-(c) depicts the peak value of the average velocity of melted PCM for unfinned and finned PV-PCM systems with different fin lengths (half fin, three-quarter fin and full fin) at various inclinations. Peak average velocity indicates the strength of the convection current that has been created inside the melted PCM. Among the different finned PV-PCM systems considered in the present study, it is clear that the velocity values are generally lowest for full fin cases, indicating a reduction of convection currents inside the PCM. In the full fin case, the resistance to the flow of melted PCM increases as the flow channel's

length is reduced and fluid friction increases, which reduces the developed buoyancy force and consequent convection current inside the PCM chamber. The velocity magnitude appears to decrease with an increase in the number of fins as the convection channel length gets reduced and fluid friction increases further.
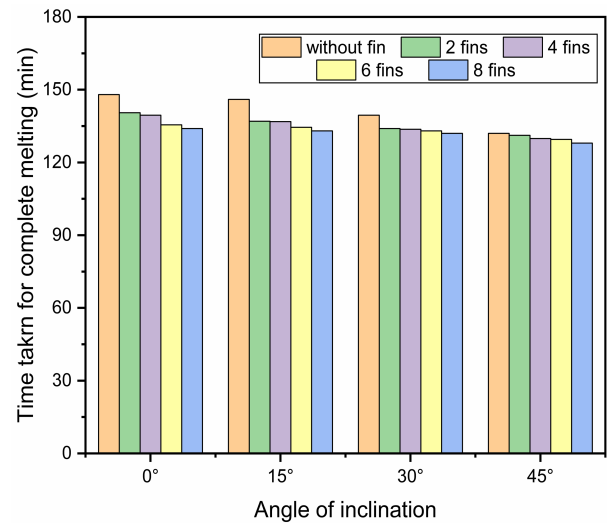

Figure 14. Comparison of melting time of PCM for all PV-PCM systems with 20 mm fin length at different inclinations.

Among all the systems with PCM, the lowest peak velocity magnitude is found in the unfinned PV-PCM system with the inclination of 0°, suggesting that convection heat transfer is insignificant and conduction is the primary heat transfer mode. As temperature differences inside the PCM rise, the peak velocity increases slightly with the number of fins for systems with 0° orientation. For inclined systems, because of the buoyancy force created within the melted PCM, the peak velocity increases as the angle of inclination increases for any fin length and number of fins. In the comparison of systems with full fin and unfinned cases, the highest magnitude of velocity is obtained as 0.61 mm/s for the unfinned PV-PCM system with the orientation of 45°. For three-quarter fin and half fin cases, the convection levels are higher than the full fin case as the flow of melted PCM can still occur through the space below the fin. The corresponding values are 0.893 mm/s for three quarter (15 mm) fin case with an inclination of 45° when the number of fins is two as well as 0.925 mm/s for half fin case (10 mm) with an inclination of 45° when the number of fins is 8.
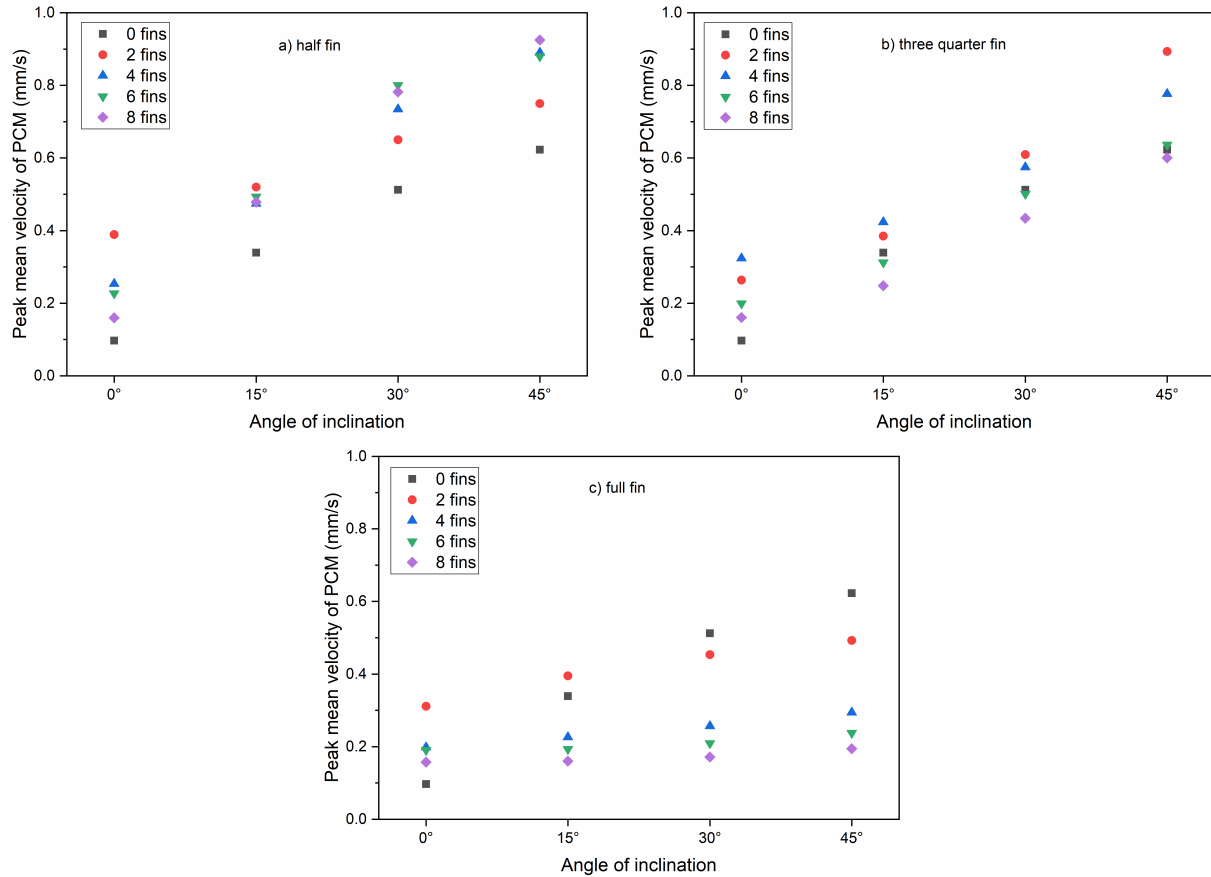

Figure 15. Comparison of peak magnitude of the velocity of melted PCM for finned PV-PCM systems at different inclinations: (a) half fin, (b) three-quarter fin, and (c) full fin.

CONCLUSIONS

The performance augmentation of the PV module, when integrated with finned PCM (RT25HC) for different numbers of fins and fin lengths, is numerically investigated at different inclinations of the system using a three-dimensional model. It is found that both increases in the number of fins and inclination angle reduce the PV temperature and thereby enhance the electrical efficiency of the PV module. Different findings of the present investigations are summarized as follows:

- The average temperature of the PV module decreases with an increase in inclination and an increase in fin length. The PV efficiency follows the opposite trend in contrast to PV temperature; PV efficiency increases with the inclination. The drop in the average temperature of the PV with the inclusion of PCM and fins is relatively highest for the finned PV-PCM system with 6 fins.

- For conventional PV-PCM systems (no fins), the maximum temperature reduction values compared to corresponding PV-only cases are 53.4°C and 43.63°C, respectively, for 0° and 45° orientations. The maximum efficiency enhancement for the corresponding orientations is 39.6% and 30.45%, respectively.

- The effectiveness of fin inclusion in the system tends to reduce with an increase in inclination.

- The effectiveness of increment in the number of fins is more prominent for full fin cases.
- The full-finned PV-PCM system with 6 fins gives a maximum PV temperature reduction of 59.65°C compared to the conventional PV-only system when the inclination is 0° among all the finned PV-PCM systems, and the corresponding maximum enhancement of efficiency is 45.1% compared to the PV-only system.
- The full-finned PV-PCM system with 6 fins and 45° inclination gives the highest instantaneous power output of 14.16 W.
- The melting rate of the PCM in the PV-PCM system is strongly influenced by inclination and number of fins, indicating the extent of the heat transfer rate within the PCM. Enhancement in melting rate with respect to increasing in inclination is due to increment in convective heat transfer rate, whereas with respect to number of fins, is due to increase in the rate of conduction heat transfer rate.
- The peak value of the average velocity of melted PCM increases with the inclination angle and decreases with the presence of fins. An increase in fin length also reduces the velocity values as it adversely affects the convection current inside melted PCM.

REFERENCES

Abdulmunem, A.R., Mohd Samin, P., Abdul Rahman, H., Hussien, H.A., Izmi Mazali, I., Ghazali, H., 2021, Numerical and experimental analysis of the tilt angle's effects on the characteristics of the melting process of PCM-based as PV cell's backside heat sink, *Renew. Energy*, 173, 520–530.

Agrawal, B., Tiwari, G.N., 2010, Optimizing the energy and exergy of building integrated photovoltaic thermal (BIPVT) systems under cold climatic conditions, *Appl. Energy*, 87, 417–426.

Akshayveer, Kumar, A., Pratap Singh, A., Sreeram Kotha, R., Singh, O.P., 2021, Thermal energy storage design of a new bifacial PV/PCM system for enhanced thermo-electric performance. *Energy Convers. Management,* 250, 114912.

Ali, H.M., 2020, Recent advancements in PV cooling and efficiency enhancement integrating phase change materials based systems – A comprehensive review, *Sol. Energy*, 197, 163–198.

Azarpour, A., Suhaimi, S., Zahedi, G., Bahadori, A., 2013, A review on the drawbacks of renewable energy as a promising energy source of the future. *Arab. J. Sci. Eng*, 38, 317–328.

Balavinayagam, K., K S, U., Rohinikumar, B., 2021, Numerical investigations on phase change material-

based battery thermal management system. *J. Phys. Conf. Ser*, 2054, 012003.

Bilen, K., Erdoğan, İ., 2023, Effects of cooling on performance of photovoltaic/thermal (PV/T) solar panels: A comprehensive review. *Sol. Energy*, 262, 111829.

Biwole, P.H., Groulx, D., Souayfane, F., Chiu, T., 2018. Influence of fin size and distribution on solid-liquid phase change in a rectangular enclosure, *Int. J. Therm. Sci.*, 124, 433–446.

Brent, A.D., Voller, V.R., Reid, K.J., 1988, Enthalpy-porosity technique for modeling convection-diffusion phase change: Application to the melting of a pure metal, *Numer. Heat Transf.*, 13, 297–318.

Bria, A., Raillani, B., Chaatouf, D., Salhi, M., Amraqui, S., Mezrhab, A., 2023, Effect of PCM thickness on the performance of the finned PV/PCM system, *Mater. Today Proc.,* 72, 3617–3625.

Chibani, A., Merouani, S., Laidoudi, H., Dehane, A., Morakchi, M.R., Bendada, L., 2023, Analysis and optimization of concentrator photovoltaic system using a phase change material (RT 35HC) combined with variable metal fins, *J. Energy Storage*, 72.

Cuce, E., Bali, T., Sekucoglu, S.A., 2011, Effects of passive cooling on performance of silicon photovoltaic cells, *Int. J. Low-Carbon Technol.*, 6, 299–308.

Cuce, E., Cuce, P.M., 2014, Tilt Angle Optimization and Passive Cooling of Building-Integrated Photovoltaics (BIPVs) for Better Electrical Performance, *Arab. J. Sci. Eng.*, 39, 8199–8207.

Da, J., Li, M., Li, G., Wang, Y., Zhang, Y., 2023, Simulation and experiment of a photovoltaic—air source heat pump system with thermal energy storage for heating and domestic hot water supply, *Build. Simul.*

Duan, J., 2021, The PCM-porous system used to cool the inclined PV panel, *Renew. Energy*, 180, 1315–1332.

Dubey, S., Sarvaiya, J.N., Seshadri, B., 2013, Temperature dependent photovoltaic (PV) efficiency and its effect on PV production in the world - A review, *Energy Procedia*, 33, 311–321.

Emam, M., Ahmed, M., 2018, Cooling concentrator photovoltaic systems using various configurations of phase-change material heat sinks, *Energy Convers. Manag.*, 158, 298–314.

Fujii, T., Imura, H., 1972, Natural-convection heat transfer from a plate with arbitrary inclination, *Int. J. Heat Mass Transf.*, 15, 755–767.
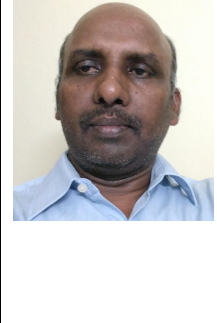
Groulx, D., Biwole, P.H., Bhouri, M., 2020, Phase change heat transfer in a rectangular enclosure as a function of inclination and fin placement, *Int. J. Therm. Sci.*, 151, 106260.

Huang, M.J., Eames, P.C., Norton, B., Hewitt, N.J., 2011, Natural convection in an internally finned phase change material heat sink for the thermal management of photovoltaics, *Sol. Energy Mater. Sol. Cells*, 95, 1598–1603.

Hui Dai, Wei-Min Ma, 2002, A novelty Bayesian method for unsupervised learning of finite mixture models, *in: Proceedings of 2004 International Conference on Machine Learning and Cybernetics (IEEE Cat. No.04EX826). IEEE*, pp. 3574–3578.

Incropera, F., Dewitt, D., 1985, *Introduction to heat transfer*, John Wiley and Sons Inc, United States.

Johnston, E., Szabo, P.S.B., Bennett, N.S., 2021, Cooling silicon photovoltaic cells using finned heat sinks and the effect of inclination angle, *Therm. Sci. Eng. Prog.*, 23, 100902.

Kaldellis, J.K., Kapsali, M., Kavadias, K.A., 2014, Temperature and wind speed impact on the efficiency of PV installations, Experience obtained from outdoor measurements in Greece, *Renew. Energy*, 66, 612–624.

Kant, K., Shukla, A., Sharma, A., Biwole, P.H., 2016, Heat transfer studies of photovoltaic panel coupled with phase change material, *Sol. Energy*, 140, 151–161.

Kaplani, E., Kaplanis, S., 2014, Thermal modelling and experimental assessment of the dependence of PV module temperature on wind velocity and direction, module orientation and inclination, *Sol. Energy*, 107, 443–460.

Kazem, H.A., Al-Waeli, A.H.A., Chaichan, M.T., Sopian, K., Ahmed, A.A., Wan Nor Roslam, W.I., 2023, Enhancement of photovoltaic module performance using passive cooling (Fins): A comprehensive review, *Case Stud. Therm.*, Eng. 49, 103316.

Khanna, S., Newar, S., Sharma, V., Reddy, K.S., Mallick, T.K., 2019, Optimization of fins fitted phase change material equipped solar photovoltaic under various working circumstances, *Energy Convers. Manag.*, 180, 1185–1195.

Khanna, S., Reddy, K.S., Mallick, T.K., 2018, Optimization of finned solar photovoltaic phase change material (finned pv pcm) system, *Int. J. Therm. Sci.*, 130, 313–322.

Khanna, S., Reddy, K.S., Mallick, T.K., 2017, Performance analysis of tilted photovoltaic system integrated with phase change material under varying operating conditions, *Energy*, 133, 887–899.

Klemm, T., Hassabou, A., Abdallah, A., Andersen, O., 2017, Thermal energy storage with phase change materials to increase the efficiency of solar photovoltaic modules, *Energy Procedia*, 135, 193–202.

Kumar, K.S., Kumar, H.A., Gowtham, P., Kumar, S.H.S., Sudhan, R.H., 2020, Experimental analysis and increasing the energy efficiency of PV cell with nano-PCM (calcium carbonate, silicon carbide, copper), *Mater. Today Proc.*, 37, 1221–1225.

Mahdi, J.M., Mohammed, H.I., Talebizadehsardari, P., 2021, A new approach for employing multiple PCMs in the passive thermal management of photovoltaic modules, *Sol. Energy*, 222, 160–174.

Metwally, H., Mahmoud, N.A., Ezzat, M., Aboelsoud, W., 2021, Numerical investigation of photovoltaic hybrid cooling system performance using the thermoelectric generator and RT25 Phase change material, *J. Energy Storage*, 42, 103031.

Mohanraj, M., Gunasekar, N., Velmurugan, V., 2016, Comparison of energy performance of heat pumps using a photovoltaic – thermal evaporator with circular and triangular tube configurations, *Building Simulations*, 9, 27–41.

Nouira, M., Sammouda, H., 2018, Numerical study of an inclined photovoltaic system coupled with phase change material under various operating conditions, *Appl. Therm. Eng.*, 141, 958–975.

Park, J., Kim, T., Leigh, S.B., 2014, Application of a phase-change material to improve the electrical performance of vertical-building-added photovoltaics considering the annual weather conditions, *Sol. Energy*, 105, 561–574.

Poirier, D.R., 1987, Permeability for flow of interdendritic liquid in columnar-dendritic alloys, *Metall. Trans. B.*, 18, 245–255.

Sasidharan, U.K., Bandaru, R., 2022, Thermal management of photovoltaic panel with nano-enhanced phase change material at different inclinations, *Environ. Sci. Pollut. Res.*, 29, 34759–34775.

Savvakis, N., Dialyna, E., Tsoutsos, T., 2020, Investigation of the operational performance and efficiency of an alternative PV + PCM concept, *Sol. Energy*, 211, 1283–1300.

Sharma, S., Tahir, A., Reddy, K.S., Mallick, T.K., 2016, Performance enhancement of a Building-Integrated Concentrating Photovoltaic system using phase change material, *Sol. Energy Mater. Sol. Cells*, 149, 29–39.

Singh, P., Khanna, S., Becerra, V., Newar, S., Sharma, V., Mallick, T.K., Hutchinson, D., Radulovic, J., Khusainov, R., 2020, Power improvement of finned solar photovoltaic phase change material system, *Energy*, 193, 116735.

Unnikrishnan, Jayatej, M., B, R., 2023, Three-dimensional numerical analysis of performance of PV module integrated with PCM and internal pin fins of different shapes, *J. Therm. Anal. Calorim.*, 148, 9739–9760.

Variji, N., Siavashi, M., Tahmasbi, M., Bidabadi, M., 2022, Analysis of the effects of porous media parameters and inclination angle on the thermal storage and efficiency improvement of a photovoltaic-phase change material system, *J. Energy Storage*, 50, 104690.

Yıldız, Ç., Arıcı, M., Nižetić, S., Shahsavar, A., 2020, Numerical investigation of natural convection behavior of molten PCM in an enclosure having rectangular and tree-like branching fins, *Energy*, 207.

	Unnikrishnan K S is currently a research scholar in the Dept. of Mechanical Engr. at the National Institute of Technology, Calicut, Kozhikode, India. He obtained his M.Tech. degree, specialising in thermal power engineering, from APJ Abdul Kalam Technological University, Kerala, in 2018. He received a B.Tech. degree in mechanical engineering from Mahatma Gandhi University, Kottayam. His current research interest focuses on the passive thermal management of PV, heat transfer, phase change material, and CFD.
	Sumanth Babu Pathipati is currently an Associate Software Engineer at IQVIA Bengaluru, India. He completed his M Tech degree, specialising in energy engineering and management, in 2022 from the National Institute of Technology, Calicut, India. He earned his B.Tech. degree in Mechanical Engineering in 2019 from VRS Engineering College, Andhra Pradesh, India. His areas of interest include heat transfer, thermal management, and energy systems.
	Dr. Rohinikumar Bandaru is currently an Asst. Prof. at the Dept. of Mech. Engr., National Inst. of Tech. Calicut, India. He obtained his PhD in Mech. Engr. from the National Institute of Technology, Calicut, India, in 2018. He has teaching experience spanning more than 20 years in the areas of thermodynamics, fluid mechanics, heat transfer, Fluid Flow and Heat Transfer in Energy Systems, Analytical Methods in Heat Transfer, Thermodynamic Property Relations and Exergy Analysis, Design and Analysis of Energy Systems and Computational Fluid Dynamics and Heat Transfer. His research interests include Fluid Flow and Heat Transfer; Experimental Investigations, Modeling, and Simulation of Solar Energy Systems; Thermal Management on Solar PV Panels; Lithium-ion battery thermal management; Thermal management of Fuel cell and Heat pipes as well as vapour chamber Modelling and refrigeration, and Air-Conditioning.